

Potentiostatic Electrodeposition as an Option to the Traditional Recovery of Silver in Artisanal Gold Smelting Wastewater in Bulacan, Philippines

Michael Vincent O. Laurio^{a,*}, Jomuel A. Velandres^a, Catalino G. Alfafara^a, Veronica P. Migo^a,
Monet Concepcion M. Detras^a, Jennifer Marie Sunga-Amparo^b, Marlo Mendoza^c

^a Department of Chemical Engineering, College of Engineering and Agro-Industrial Technology, Andres P. Aglibut Ave., University of the Philippines Los Baños, College, Laguna 4031 Philippines

^b College of Human Ecology, University of the Philippines Los Baños, College, Laguna 4031 Philippines

^c College of Forestry, University of the Philippines Los Baños, College, Laguna 4031 Philippines

Abstract – Potentiostatic electrodeposition for silver recovery in the artisanal gold smelting of Bulacan, Philippines was investigated as an alternative cost-effective method to prevent the generation of copper nitrate-rich effluent. The electrodeposition of dominant metal ions (silver, copper, iron, and lead) were observed from time-course profiles of metal ion removal efficiencies and measured currents at varying constant operating voltages. Initial silver ion removal rates increased with operating voltage supplied, however, redissolution also occurred during high-potential operation (1.5V to 2.0V). The occurrence of co-deposition and redissolution was managed by determining critical electrodeposition conditions. A critical operating voltage of 1.33 V favored high silver purity from recovered deposits at 89.5%, while critical electrodeposition time minimized the occurrence of metal redissolution under high-potential conditions. At an optimum voltage of 1.66 V, the observed silver ion removal was 77.8% and the silver purity from recovered deposits was 86.5%. Finally, the charge dose scale-up parameter was 0.528 C/mg silver ion removed and the corresponding energy requirement was 0.24 kWh/kg silver ion removed. Considering the increased silver purity from recovered deposits, and the lower charge dose and energy requirement, this study presents some advantages of potentiostatic electrodeposition in artisanal gold smelting.

Keywords: electrodisposition, gold smelting, silver nitrate, scale-up, charge dose

I. INTRODUCTION

Gold recycling from used jewelry and scrap electronic circuit boards is one of the flourishing industries in the Bulacan province, Philippines, and has been considered as a potential source of heavy metal pollution of the Marilao-Meycauayan-Obando (MMO) river system. Since 2008, the river system has been an environmental hotspot for water quality [1], [2] from local industrial heavy metal pollution [3], [4] that contaminate several of its aquaculture industries [5]-[7]. Gold smelting in the municipality employs silver amalgamation, unlike conventional gold extraction methods that use mercury or cyanide [5]-[7]. In the process, used jewelry and scrap electronic circuit boards are first thermally melted with silver to separate metal impurities and form a gold-silver amalgam. Concentrated nitric acid is then added to dissolve the amalgam to separate high-purity gold nuggets while generating a silver-nitrate-rich wastewater. As a treatment method, local smelters recover silver from the wastewater by immersing copper bars to displace silver ions into silver metal. This reaction oxidizes copper into its ionic form and generates a copper-nitrate-rich effluent. Artisanal gold smelters lack the facilities to treat the toxic fumes and wastewaters generated from the process [8], and the unregulated discharge of effluents has become a common practice

that led to copper pollution [14], [15]. Copper pollution disrupts the ecological processes of the river system [9]–[11], degrades the livelihood of local fish farmers [12]–[14], and poses health risks from copper-contamination [15]. As a response, the local government has strengthened its pollution control policies in rehabilitating the MMO river system [16]–[18]. Initially, point-source reduction measures via alkali precipitation and electrodeposition of the copper-rich effluent were found effective treatments for removing copper and other heavy metals from the gold smelting effluent [7]. However, despite the effectiveness of these methods, supplemental treatments for copper hydroxide sludge management, pH adjustments were still necessary for regulatory compliance.

Silver recovery routes that avoid the generation of copper-rich effluents are seen as more attractive solutions. However, conventional industrial methods such as chemical reduction [23, 24], solvent extraction [25, 26], and photocatalytic approaches [23] in semiconductor wastes and spent catalyst treatment, use chemical agents and generate secondary effluents that need further treatment. Alfafara et al. [6] investigated the electrodeposition technique as a means to recover silver from the gold smelting effluent directly. At applied constant currents, silver ions from the effluent reduce to metal deposits on stainless-steel cathode. The process has high removal efficiency with an estimated operating cost of PhP 121/m³ (about \$3/m³) of silver-rich effluent [6]. This cost was three times less expensive than that expected in electrochemically treating the copper-rich effluent at about \$11.47/m³ of the wastewater treated [7]. Despite the advantages, the electrodeposition method still requires improvement as metal contaminants from the gold smelting effluent affect the quality of silver recovered from the process [6]. Operating voltages vary and influence a variety of electrochemical reactions during “galvanostatic” or constant-current electrodeposition. These reactions include the deposition of metal contaminants in the gold smelting wastewater, thus, affecting the purity of the recovered metal deposits [6]. Metal impurities lower the current efficiency of the process that results to additional operating costs as these conditions employ excess operating voltages that increase the energy requirement of the process [7].

Constant-voltage or “potentiostatic” electrodeposition may improve the current efficiency of silver recovery at lower the electrodeposition costs. Under a uniform applied potential, stable current densities tend to control the electrochemical reactions affecting the morphology, structure, crystallinity, conductivity, and purity of the deposits [24]. Apart from the operating voltage, other factors have also been explored in literature to control the yield of potentiostatic electrodeposition. Studies show that the morphology of electrodeposited metals depends on the level of pH where highly acidic conditions tend to influence the dendritic nature and roughness of metal deposition [25], [26]. The thin-film deposition brought about by higher levels of pH may improve of current efficiencies and electrodeposition rates that could further enhance the yield of silver recovery [27]. Similarly, the influence of electrode material on charge transport has been one of the areas of study for surface-controlled industrial products such as semiconductors [28], [29]. The effect of temperature also correlates the kinetics of the electrochemical reactions that simultaneously occur during the process [30]. Overall, potentiostatic electrodeposition is common in industrial electronic applications on semiconductors [30 – 33], energy storages [34, 35], electrocatalysis [36, 37], nanomaterial synthesis [39], and photovoltaic cells [39 – 42] to control the quality of product and process

performance. However, the application of the potentiostatic technique on metal recovery in a wastewater treatment setting has so far been limited. The differences in the properties of industrial streams tend to be extensive that specific operational differences would make direct comparisons difficult. Also, most studies found in the literature compare the performance of potentiostatic and galvanostatic electrodeposition. Few had taken consideration of optimizing the conditions in recovering valuable metals from effluents. Thus, this study proposes a potentially less expensive silver recovery alternative for small-scale gold smelting operators in Bulacan, Philippines. Electrodeposition time profiles for residual metal ion concentrations and measured currents at different constant operating voltages were analyzed and correlated with silver recovery and purity. An optimum operating voltage was also determined from these correlations. Finally, a charge dose scale-up parameter was determined to estimate the cost of potentiostatic electrodeposition in comparison with that of the galvanostatic mode.

II. MATERIALS AND METHODS

2.1 Preparation of Gold Smelting Wastewater

The silver-nitrate-rich effluent was obtained from a local gold smelting plant in Meycauayan, Bulacan, Philippines (stream D from the quenching process as shown in **Figure 1**). The sample was initially analyzed for metal concentrations of silver, copper, lead, and iron using a PerkinElmer AAnalyst 400 Atomic Absorption Spectrophotometer (AAS) [44]. These four metals were considered as the dominant metals based on the elemental analysis done on cathode deposits using a Niton XL3t X-ray Fluorescence (XRF) analyzer.

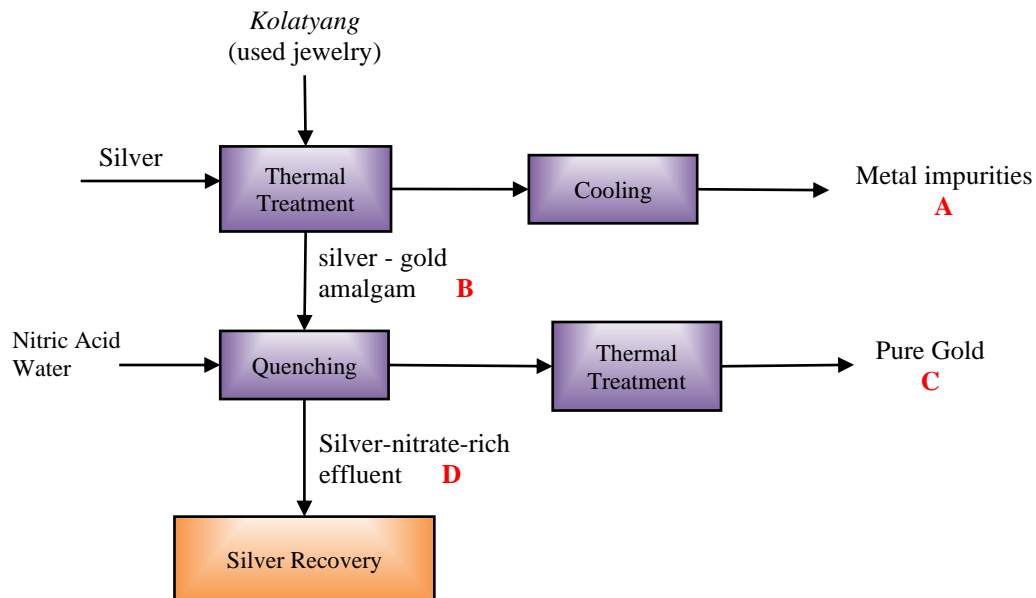


Figure 1. Simplified block diagram of the traditional gold smelting process of Bulacan, Philippines based on used gold jewelries, showing relevant process streams, with stream D as the wastewater used in the experiments.

2.2 Experimental Set-up

A batch electrolysis set-up (**Figure 2**), was used for the electrodeposition experiments. A working volume of 400 mL was considered for the set-up. Electrodes measuring 5 cm x 15 cm each were placed in the reactor (500-mL tall beaker), with a 4-cm spacing provision. The stainless-steel cathode was chosen for its local availability and low cost that would decrease the capital cost of the electrodeposition set-up when scaled-up. The sintered platinum anode was a reusable inert electrode that was seen to have high compatibility for electrodeposition studies conducted in gold smelting wastewaters [6], [7]. The low cost and reusability of these electrodes make them an economically attractive choice, especially for artisanal gold smelting operations such as that found in Bulacan, Philippines. The electrode package was held together using Teflon® tape and rubber spacers. Different values of constant operating voltage was supplied from a direct current power source (WSPS-817 DC Power Supply, Wheeler). The electrodes are immersed such that each would have an electrode surface area of 75 cm² available for electrochemical reactions. A magnetic stirrer mixed the wastewater. The negative terminal (black outlet) of the power source was connected to the cathode, while the anode was fixed to the positive terminal (red outlet). For a constant amount of voltage supply, the changes in voltage and current were monitored using digital multi-meters wired to the set-up. All runs were conducted in duplicate. Lastly, for comparison, a constant-current electrodeposition experiment at 9 A was also performed and evaluated in terms of purity of silver, copper, iron, and lead in the recovered metal deposits.

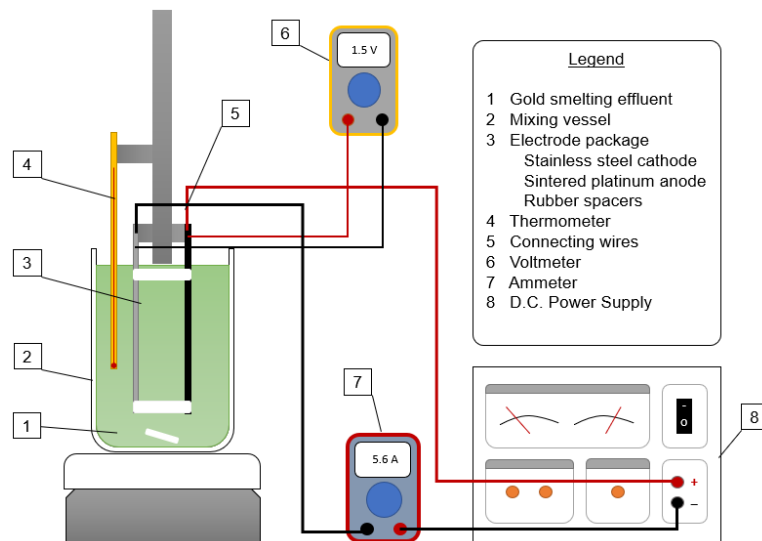


Figure 2. Schematic diagram of electrodeposition set-up

2.3 Evaluation of Electrodeposition Performance

Initially, electrodeposition time-profile experiments were conducted for 180 min at varying values of constant operating voltages between 1 V to 2 V, according to the operational limitations of the DC power source. Despite the limitation, currents up to 10 A were measured from the operating voltages. These currents ensure that electrochemical reactions for silver and other metals would proceed based on previous constant-current electrodeposition studies where a maximum applied current of 9A was employed [6]. These currents were directly

measured from digital multi-meters at 20-minute intervals, and 5-mL of electrolyzed samples were obtained. Current densities were also calculated by dividing the measured current by the initial surface area of the stainless-steel cathode. The samples were then analyzed for residual silver, copper, lead, and iron ion concentrations. The residual metal ion concentrations were used to determine metal ion removal efficiencies using Equation 1:

$$\% \text{ removal efficiency} = \frac{(C_o - C)}{C_o} \times 100 \quad (1)$$

At the end of each run, the cathode deposits, i.e., all recovered silver-rich metal deposits attached and dislodged from the stainless-steel cathode, were obtained, oven-dried at 90°C for three hours, and then weighed to obtain the masses of the metal deposits. The overall mass of the deposits was considered in all mass calculations. At this point, silver purity was not determined yet.

As will be discussed in Section 3.4, a critical electrodeposition time (t_{critical}) was correlated with operating voltage from time-course profiles. Electrodeposition experiments were conducted at different values of constant operating voltages between 1.5 and 2.0 V and at correlated values of t_{critical} to determine the effect of high potential operation on metal ion removal efficiency, purity of cathode deposits, and metal recovery efficiency. The cathode deposits were collected, dried, weighed, then dissolved in nitric acid. The dissolved deposits were then diluted accordingly for silver, copper, lead, and iron analyses via AAS. These concentrations were used to calculate the purity of the cathode deposits with respect to each metal species analyzed, using Equation 2:

$$\% \text{ purity} = \frac{(C_d)(V_s)}{W_d} \times 100 \quad (2)$$

The purity of the deposits was used to determine the corresponding silver recovery efficiency relative to the initial mass of silver in the effluent, and from the product of initial metal concentration and an initial working volume (Equation 3):

$$\% \text{ recovery} = \frac{W_d}{(C_o)(V_m)} \times \% \text{ purity} \quad (3)$$

The effects of operating voltage on metal removal efficiencies, mass and purity of deposits, and silver recovery efficiency were analyzed and correlated with the aid of statistical software Design Expert v11 (SN: 4156-3030-4752-8487). Model equations were generated to correlate the effects of operating voltage on process responses such as metal removal efficiencies, silver recovery efficiency, and the mass and purity of recovered deposits. These model equations were used to determine the optimum operating voltage that can be further scaled-up.

2.4 Determination of Charge Dose and Energy Requirement

A scale-up parameter was determined based on the amount of electrical charge that is needed to electrochemically remove a unit mass of the silver from the gold smelting effluent, also known as the charge dose parameter. This was empirically determined using Equation 4:

$$It = Q(C_0 - C) V \quad (4)$$

From Equation 4, the charge dose was estimated from the linear plot between the electrical charge [It] versus the mass of the electrochemically removed metal species [(C₀-C) V_m]. As a scale-up parameter, the charge dose may also be used to determine the corresponding energy requirement (kWh/mg silver) for the electrodeposition process at constant voltage. This energy requirement was calculated using Equation 5.

$$\text{Energy Requirement} \left(\frac{\text{kWh}}{\text{mg silver}} \right) = \frac{1}{3.6 \times 10^6} QE \quad (5)$$

The estimated energy cost for the electrochemical recovery operation was calculated by multiplying the energy requirement by the prevailing local electricity cost.

III. RESULTS AND DISCUSSION

3.1 Characteristics of the Gold Smelting Wastewater

The gold refining process in Bulacan, Philippines is based on a hydrometallurgical process that is most suitable on high-gold alloys such as scrap gold jewelries [45]. Silver is melted with the scrap gold jewelries where silver forms an alloy or amalgam with gold. The silver-gold amalgam is quenched with nitric acid to dissolve silver while gold forms insoluble residues, called nuggets. Ideally, the silver-gold amalgamation step is a selective process. However, the generally uncontrolled operating conditions in artisanal gold extraction (process temperature, relative amounts of chemical reagents, reaction time, etc.) resulted in metallic impurities in the effluent. AAS results shown in **Table 1**, present silver as the dominant metal in the wastewater, along with copper, lead, and iron in relatively trace concentrations.

3.2 Purity of Silver Deposits Under Galvanostatic Electrodeposition

Silver and other metals also showed co-deposition under constant current electrodeposition at 9 A based on the analysis of recovered metal deposits (**Table 1**). Under this condition, the recovered deposits have a silver purity of about 79.1%, while metal co-deposits from copper, and traces of iron and lead totaled to about 3.64%. Non-metal impurities of sulfur and potassium were also present in the deposits at 16.87%. The presence of impurities under high-current operation indicates excessive voltages that may have influenced metal co-deposition. This results in lower current efficiencies relative to silver recovery that leads to higher energy costs [7]. Low-purity silver reused for extracting gold may also affect gold recovery efficiencies and quality. For considerations of lower cost and better purity of deposits, the study further investigated potentiostatic electrodeposition as an alternative approach for silver recovery.

Table 1. Dominant metal species present in the gold smelting effluent, and composition of metal deposits recovered from galvanostatic electrodeposition.

SPECIES	COMPOSITION	
	Effluent ^a (mg/L)	Deposits ^b (%)
Silver (Ag)	371,622	79.11
Copper (Cu)	19,210	2.44
Lead (Pb)	2,917	0.18
Iron (Fe)	43	1.02
Non-metal species (Sulfur and Potassium)		16.87

a AAS analysis of raw gold smelting effluent

b XRF analysis of metal deposits obtained under galvanostatic electrodeposition at 9 A.

3.3 *Potentiostatic Electrodeposition Time-Course Profiles*

Time profiles for metal ion removal efficiencies of silver, copper, lead, and iron, and

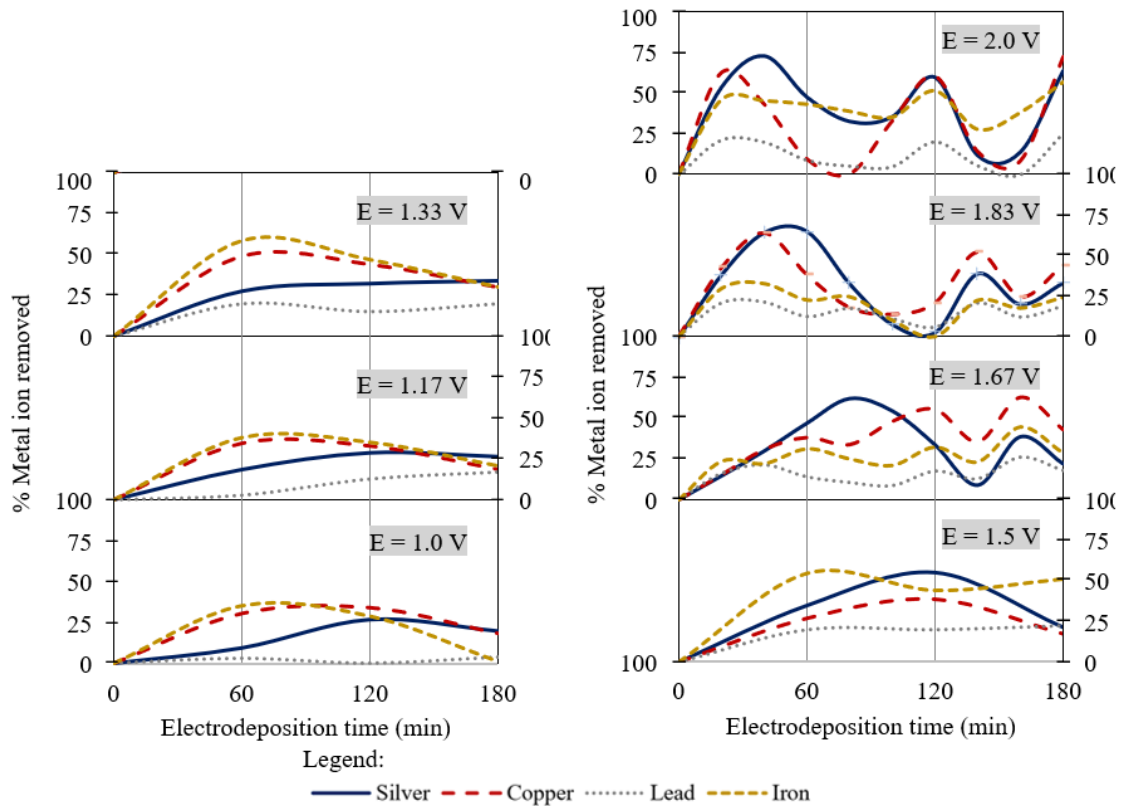


Figure 3. Electrodeposition time course profiles of percent metal ion removal for silver, copper, lead, and iron under various constant operating voltages

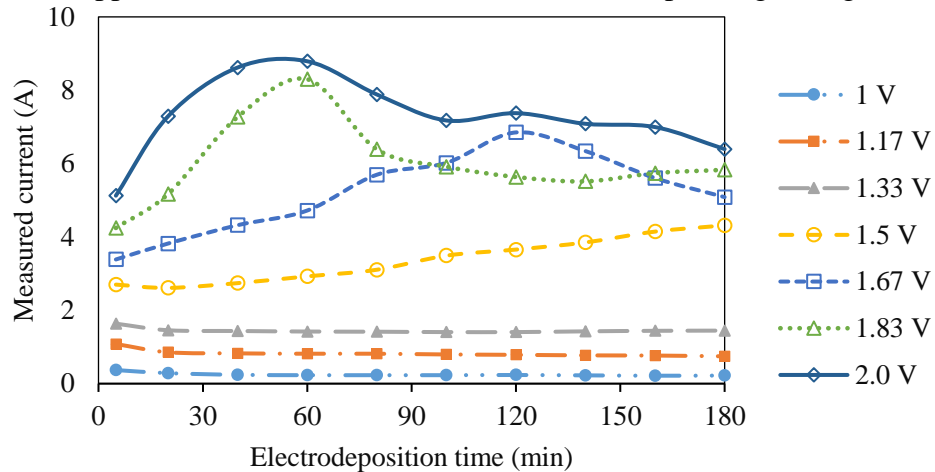


Figure 4. Electrodeposition time course profile of measured currents under various constant operating voltages

Observations from the electrodeposition experiments are also presented in **Figure 5**. At the start of the process, sand-like silvery metal deposited onto the stainless-steel cathode while bubbling on the sintered platinum anode with a faint nitric oxide (NO) odor were observed. These indicated the reduction of silver ions into silver metal at the cathode, and oxidation of water and possibly of nitric acid into gases at the anode. The increase in percent removal of silver, copper, lead, and iron ions in the time profiles indicates their co-deposition at the cathode surface.

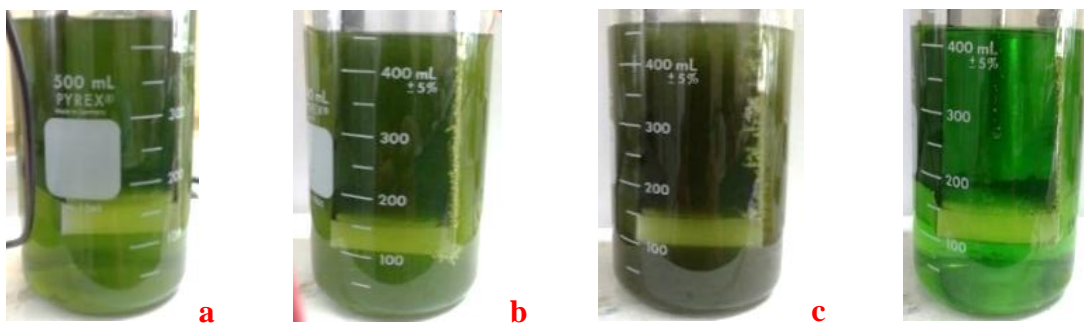


Figure 5. Observations during experimental electrodeposition process at various operating voltages: (a) thin layer of sand-like silvery deposits on cathode with few bubbling at the anode and weak scent of nitrogen oxide throughout electrodeposition at 1.0 V to 1.33 V, and only during the start of electrodeposition at 1.5 V to 2.0 V; (b) uneven or dendritic silvery deposits on cathode with more bubbling at the anode and stronger scent of nitrogen oxide during electrodeposition at 1.5 V to 2.0 V; (c) formation of black particulates during electrodeposition at 1.5 V to 2.0 V; and (d) disappearance of cathode deposits at extended electrodeposition time.

Reduction potentials (E_{cell}), presented in **Table 2**, were also considered to identify the possible reactions in the stainless-steel cathode and sintered platinum anode during electrodeposition. Chemical species that have more positive cell potentials tend to have a higher affinity for electrons to reduce to the metal state. In contrast, those that have more negative cell potentials tend to lose electrons and undergo oxidation [46]. Silver was the dominant metal ion removed during electrodeposition, as its high concentration in the effluent favored its affinity for electrons influencing its reduction into the metallic state ($E_{\text{cell}} = 0.80$ V). The reduction of copper ions followed next based on its standard reduction potential of 0.34 V. The relative values of the reduction potentials of lead ($E_{\text{cell}} = -0.13$ V), and iron ($E_{\text{cell}} = -0.44$ V) indicate that these metal ions are least likely to be electrodeposited. A higher potential is required for them to be deposited on the stainless-steel cathode. However, as the electrodeposition set-up was only a two-electrode system, reduction potentials were estimated from the Nernst equation using the concentrations of metal ions in the time course. In contrast, a three-electrode system involving an additional reference electrode offers higher stability in accurately measuring potentials in electrochemical systems. This set-up is recommended for further detailed parametric studies.

Table 1. Electrochemical Reactions from the Gold Smelting Effluent.

OBSERVATION	POSSIBLE REACTIONS	E_{cell} (V)
Bubbling at the surface of the electrodes	Reduction: $2\text{H}^+_{(aq)} + 2\text{e}^- \rightarrow \text{H}_{2(g)}$	0.00
	Oxidation: $4\text{OH}^-_{(aq)} \rightarrow \text{O}_{2(g)} + 2\text{H}_2\text{O}_{(l)} + 4\text{e}^-$	- 0.40
Formation of sand-like and dendritic deposits onto the cathode	Reduction: $\text{Ag}^+_{(aq)} + \text{e}^- \rightarrow \text{Ag}_{(s)}$	0.80
	Reduction: $\text{Cu}^{2+}_{(aq)} + 2\text{e}^- \rightarrow \text{Cu}_{(s)}$	0.34
	Reduction: $\text{Pb}^{2+}_{(aq)} + 2\text{e}^- \rightarrow \text{Pb}_{(s)}$	- 0.13
	Reduction: $\text{Fe}^{2+}_{(aq)} + 2\text{e}^- \rightarrow \text{Fe}_{(s)}$	- 0.44
Formation of black suspended deposits	Oxidation: $\text{Ag}_{(s)} + \text{S}^{2-}_{(aq)} \rightarrow \text{Ag}_2\text{S}_{(s)}$	- 0.69
Re-dissolution of metal deposits, e.g. Ag	$3\text{Ag}_{(s)} + 4\text{HNO}_{3(aq)} \rightarrow 3\text{AgNO}_{3(aq)} + \text{NO}_{(g)} + 2\text{H}_2\text{O}_{(l)}$	
	$3\text{Ag}_{(s)} + 2\text{HNO}_{3(aq)} \rightarrow \text{AgNO}_{3(aq)} + \text{NO}_{2(g)} + 2\text{H}_2\text{O}_{(l)}$	
	$4\text{H}^+_{(aq)} + \text{NO}_3^- + 3\text{e}^- \rightarrow \text{NO}_{(g)} + 2\text{H}_2\text{O}_{(l)}$	0.96

The measured currents increased with operating voltages (**Figure 4**), and favored higher initial silver ion removal rates (**Figure 6**), following Ohm's law. The calculated average current densities based on initial cathode surface area also increased with operating voltages from 0.33 A/m² at 1.0 V, to 9.80 A/m² at 2.0 V. For "low" operating voltages (< 1.33 V), the measured currents approached nearly constant values, indicating the constant combined resistances of the electrode and deposits. Consequently, uniform, thin layers of sand-like deposits were observed on the surface of the stainless-steel cathode (**Figure 5a**) indicate that the depositing ions have sufficient time to conform in low-energy morphological configurations [24]. At "high" operating voltages (1.5 V to 2 V), dendritic or branched cathode deposits formed, some of which were detached as the sample was mixed (**Figure 5b**). The

measured currents increased and reached peak values before gradually decreasing in order to conform a constant potential during electrodeposition. This trend indicates the two stages commonly observed in potentiostatic electrodeposition [43]. The current initially increases during the nucleation or build-up of deposits and reaches a maximum current as the cathode surface is fully covered with deposits. At this point, the high potential supplied and the increase in current, hence current densities, influenced the dendritic deposition behavior since the time for the depositing ions to conform into low-energy configurations was not enough [24]. However, the deposition behavior tend to increase the surface area of the electrode that result in the decrease of current densities. The measured currents further decreased as a result of the increase in the combined resistances of the deposits and cathode.

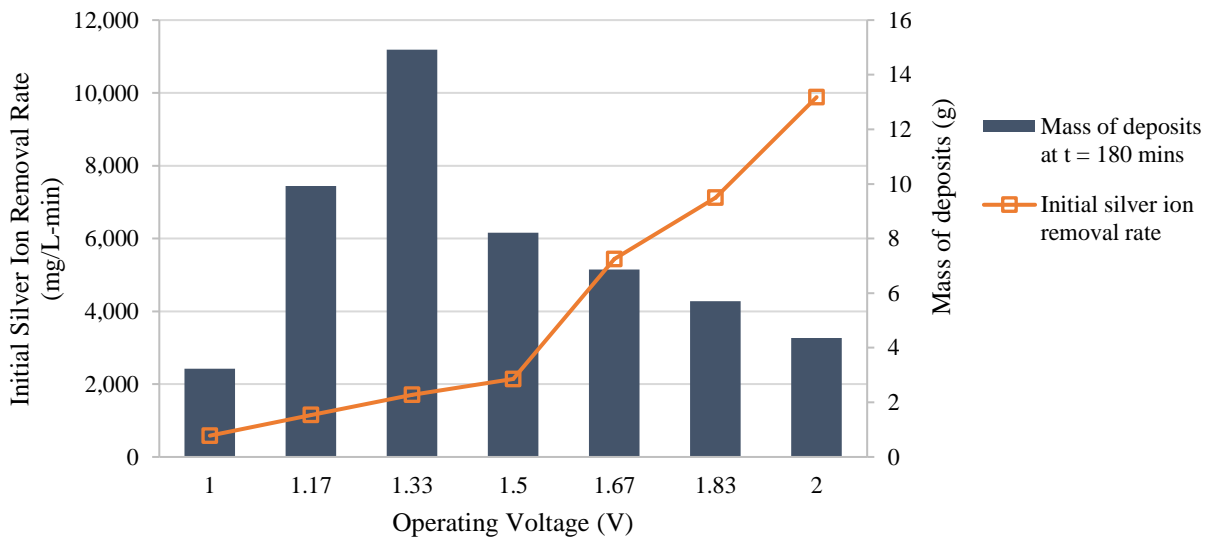


Figure 6. Calculated initial rate of silver ion removal, and measured mass of cathode deposits (after 180 minutes) from the electrodeposition of silver-rich gold smelting wastewater under various constant operating voltage conditions (1V to 2V).

Suspended black particulates also appeared in the effluent as the current increased throughout the electrodeposition time (**Figure 5c**). These black particulates were observed during galvanostatic electrodeposition at 9 A that were initially suspected as trace metal impurities of copper [6]. Oxides of the metals may have also formed during deposition that may affect the purity of the deposits that may be verified from compositional analysis, e.g. by X-ray Diffraction (XRD). However, XRF analyses of the cathode deposits show that the black deposits may be metal sulfides. Prahbune et al. [47] showed that thin films of silver sulfide can also be electrodeposited onto stainless-steel substrate via potentiostatic electrodeposition with silver nitrate and thiosulphate acting as precursor sources. Omeiri et al. [48] also confirmed a similar electrochemical formation of silver sulfides according to the chemical reaction shown in **Table 1**.

Metal ion removal efficiencies progressed from gradual single peaks at low operating voltages (1.0 V to 1.5 V), to sharp multiple periodic peaks at high operating voltages (1.66 V to 2.0 V) in the time-course profiles. This trend indicates the simultaneous reduction and

dissolution of the metals during the process. Also, measured currents unexpectedly decreased as deposits start to dissolve (**Figure 5d**). The dissolution of cathode deposits was evident based on the decreased amounts of cathode deposits collected after 180 minutes for operating voltages between 1.5 V and 2.0 V (**Figure 6**). Under low operating voltages, the silver ion removal efficiency was only about 30% after 180 minutes, indicating that the amount of current supplied led to low removal rates at the expense of long electrodeposition time. According to Ozmetin [30], the dissolution of silver metal in nitric acid can be catalyzed in nitrous acid that can be formed in the electrochemical process. Electrochemical reactions in nitric acid solutions with voltages above 0.96 V (versus standard hydrogen electrode) reduce the nitrate ions (NO_3^-) into nitrous ions (NO_2^-) at higher rates than cathodic deposition especially as the supply of current increased [49]. These reactions are autocatalyzed in concentrated nitric acid solutions and under excessive operating voltages, and the various mechanisms presented in literature show the complex nature of the reactions that must be further investigated [50]. Electroanalytical methods employing cyclic voltammetry is recommended to verify the mechanism of these reactions in the gold smelting effluent [48].

While the operating voltage primarily serves as the driving potential for electrochemical reactions, other factors tend to affect the electrodeposition behavior. The influence of pH and electrode type on the morphology of deposits may address the dendritic nature and roughness of the silver deposits [27], [51]. The effect of temperature on the dissolution of silver during electrodeposition may also be investigated as this factor directly correlates the kinetics of the electrochemical reactions that simultaneously occur during the process [30]. Considering these factors may lead to improved current efficiencies and yield of silver recovery. However, this study was limited on investigating the effects of operating voltage to minimize the added costs in the operation. Considerations for pH adjustment, electrode replacement, and temperature control in electrodeposition may influence the economics of the process for small-scale operators. Nonetheless, their effects on the simultaneous electrodeposition of metals from the gold smelting wastewater may also be considered for future detailed parametric studies.

The study provided an insight into the electrodeposition behavior of the gold smelting wastewater from a simplified electrochemical set-up, using time-course profiles. However, the reaction mechanisms of the process may be best understood using electroanalytical methods such as cyclic voltammetry [48]. These approaches are highly recommended in detailed parametric studies. Despite the limitations, the observations, so far, present challenges in optimizing the potentiostatic electrodeposition technique, as increasing the operating voltage does not necessarily lead to high-purity of silver deposits due to the co-deposition of other metals. Also, the redissolution of metal deposits at prolonged potentiostatic electrodeposition prevents the operation from achieving high silver ion removal efficiencies and complete silver recovery. While operating at low potential seems to minimize the unwanted reactions, the slow rate of metal ion removal would only require longer electrodeposition time. Because of the distinct limitations observed from low and high potential electrodeposition experiments, a suitable operating voltage that minimizes the redissolution reactions at minimum electrodeposition time was also experimentally determined.

3.4 *Critical Potentiostatic Electrodeposition Conditions*

The concurrence of peak removal efficiencies and measured currents is a common observation in electrodeposition where the voltage supplied is in excess of the Nernst potential of the desired reaction, resulting in the changes of measured currents [32]. In this study, peak currents from time-course profiles were observed for each operating voltage to establish critical conditions to minimize metal dissolution during electrodeposition. These include (a) the critical voltage that show the transition of observed results from low- and high-potential operations; and (b) the critical electrodeposition time (t_{critical}) that define the extent of electrodeposition runs where the redissolution of cathode deposits can be minimized under high potential conditions. An equation analogous to that used in saturation kinetics [52] was used to correlate t_{critical} with operating voltage, as shown in Equation 6:

$$t_{\text{critical}} = \frac{a(E)}{b + E} \quad (6)$$

The experimental values for t_{critical} and corresponding operating voltage were used to determine the empirical constants ($a = 883.2$ s (14.72 min), and $b = -1.33$ V). The voltage constant (b) denotes that the equation may only be applicable for predicting t_{critical} for operating voltages above 1.33 V. This also suggests a critical voltage condition that can serve as a basis for distinguishing low- and high-potential electrodeposition mechanisms (rates of removal, structure of deposits, deposition, redissolution, etc.).

Potentiostatic electrodeposition of gold smelting effluent containing 63,500 ppm silver was conducted at the critical potential of 1.33 V for 180 minutes. The corresponding initial rate of silver ion removal was found to be 305 ppm/min. This was relatively lower than the estimated removal rate observed in **Figure 5**, which was around 1,706 ppm/min. However, this difference was reasonable and proportional to the initial concentration of silver at about 371,600 mg/L. On the other hand, the purity of the cathode deposits was 89.33% and was substantially higher than that obtained under constant current (9A) electrodeposition, at approximately 79.1%. This shows that competing reactions still occurred even at the critical voltage of 1.33 V but only up to a certain extent. These reactions include the reduction of silver ion and other metal ion impurities into metal deposits. Also, the formation of nitrous ions could have occurred that may precursor the dissolution of the co-deposited metals at electrodeposition time. It is likely that these reactions may also occur at operating voltages higher than 1.33 V. However, this was minimized by considering the calculated critical time in the electrodeposition parameters. This higher purity shows that low potential electrodeposition improves the silver recovery operation in terms of the quality of cathode deposits. However, it should also be noted that this required 180 minutes to obtain around 84.37% silver recovery efficiency. This electrodeposition time is substantially long and requires higher scale-up design and capital costs. Thus, the electrochemical recovery process under high-potential conditions was further investigated in an attempt to increase the electrodeposition rate, and thereby shorten the electrodeposition time.

3.5 Effects of High-Potential Operation at Critical Electrodeposition Time

The effects of high-potential electrodeposition of the gold smelting effluent (1.5 V to 2.0 V) on metal ion removal efficiencies, and purity of cathode deposits obtained at

corresponding critical electrodeposition time were investigated and the results are shown in **Figures 7a** and **7b**, respectively.

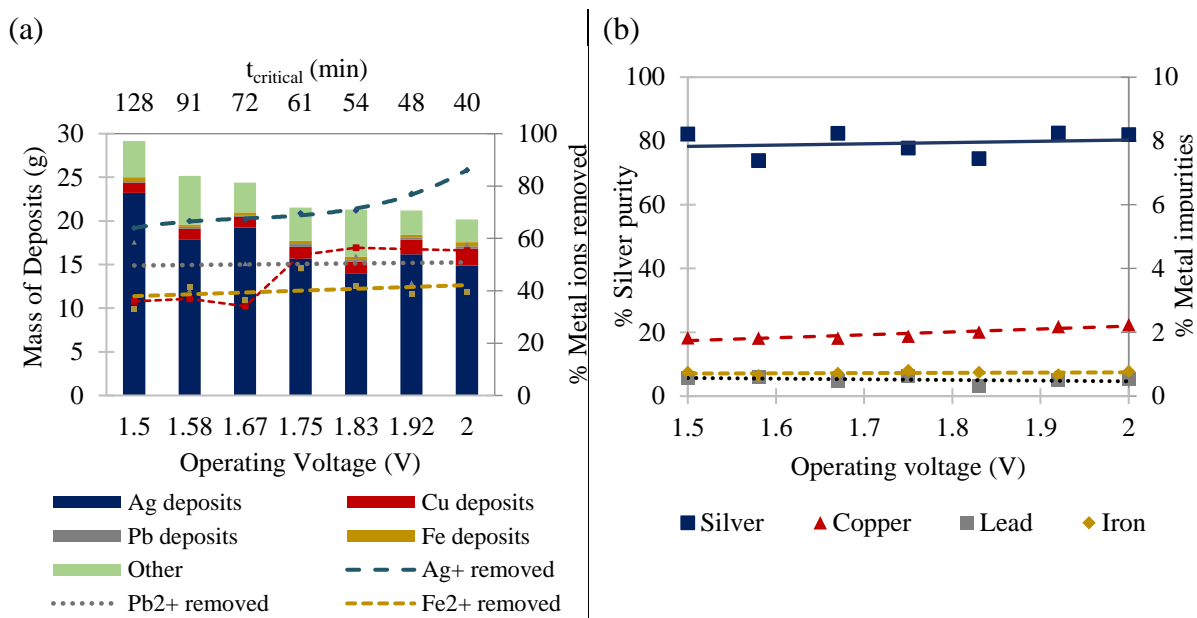


Figure 7. Characteristics of metal deposits and metal ion removal from the electrodeposition of silver-rich gold smelting wastewater under various operating voltages at calculated critical electrodeposition time: (a) mass of deposits recovered versus percent silver ion removed; (b) purity of metal deposits.

An increase in removal efficiencies with operating voltage was observed for silver and copper ions from 64% to 86%, and 33% to 56%, respectively, while those of lead and iron ions were essentially invariant and averaged to about 50% and 40%, respectively. This shows that the relatively higher reduction potential and initial concentrations of silver and copper in comparison to lead and iron favored their deposition onto the stainless-steel. Also, the increase in measured current at higher electrodeposition potential further resulted in faster reaction rates.

The silver purity from the recovered metal deposits at different levels of high operating voltages ranged from 74% to 82%. These values were found to be statistically invariant with the operating voltage indicating an average purity of about 81.7%. This purity was lower than that obtained under 1.33 V indicating that the high operating voltage influenced more competing reactions to occur. Metal impurities attributed to copper, iron, and lead deposits corresponded to 3.3%, while the remaining 18.5% were attributed to sulfur and potassium impurities. Similar to silver purity, these impurities were found to be statistically invariant with operating voltage. This trend indicates the uniform electrodeposition of metals onto the cathode surface regardless of applied potential. However, according to Hanafi, et al. [53], while purity is uniform, only the structure of the deposited metals tends to vary with operating voltage. While the measured current increased the deposition kinetics with higher electrodeposition potentials, more rapid growth in particle size results in a more dendritic

deposition behavior. This behavior makes potentiostatic electrodeposition suitable for electrodepositing uniform metal alloy films where highly controlled structures are required.

The masses of the deposits recovered from the process at the corresponding critical electrodeposition times were higher than those obtained at extended electrodeposition of 180 mins. This shows that the redissolution of the cathode deposits was minimized by predicting the critical electrodeposition parameter. However, despite this consideration, the redissolution of silver and other metal deposits at higher operating voltages still occurred based on the decreasing mass of cathode deposits, shown in **Figure 7a**. As a result, the mass of cathode deposits, hence the overall silver recovery efficiencies at higher operating voltages were lower compared to what was expected from the percent silver ion removal. The deviation of silver metal recovery increased under higher operating voltages indicating that the rate of silver redissolution overcomes that of silver metal deposition. This happens as the reduction potential for the latter was lower than that influencing the conversion of nitrates into nitrous ions. This presents an economic disadvantage for high potential operations.

3.6 *Optimal Condition for High-Potential Electrodeposition*

The potentiostatic electrodeposition experiments, so far, reflect the complex deposition behavior of different species over time. While operating voltage highly dictates the efficiency of the process in recovering silver, the varying composition of the components of the gold smelting wastewater tends to make the process difficult to predict. However, the approach of electrodeposition experiments implemented in this study limits the actual reactions that may be correlated to predict the mechanism and performance of the process in determining the optimum conditions. Despite the limitations, an alternative optimization approach was used by statistically correlating the effects of operating voltage on process responses such as metal removal efficiencies, silver recovery efficiency, and the mass and purity of recovered deposits. With the aid of Design Expert v11, model regression was performed based on statistical tests for model significance, lack-of-fit, and desirable coefficients of determination (R-squared). The results showed that only the operating voltage had a statistically significant effect on silver ion removal efficiency, copper ion removal efficiency, mass of deposits, and silver recovery efficiency. Uncoded model equations were generated (as shown in Equations 7 to 9) and may be numerically solved to determine an optimum voltage for scale-up operation.

$$\% \text{ Ag Removed} = 291.48 - 295.14 E + 96.01 E^2 \quad (7)$$

$$\text{Mass of Deposits} = 177.38 - 160.45 E + 40.51 E^2 \quad (8)$$

$$\% \text{ Ag Recovered} = 119.58 - 40.10 E \quad (9)$$

In the interest of selectively recovering silver from the gold smelting effluent, numerical optimization was employed with the aid of the statistical software where the goal was to maximize silver ion removal efficiencies, silver recovery efficiency, and mass of deposits. The resulting optimum voltage was 1.66 V. Experimental verification was performed at an optimum voltage of 1.66 V for a calculated critical electrodeposition time of 72.1 minutes to compare the predicted and actual responses of the process.

Table 2 shows a summary of the results of experimental verification.

Table 2. Results of Experimental Verification of Electrodeposition of Silver Under Optimum Operating Voltage of 1.66 v.

RESPONSE	UNIT	PREDICTED	ACTUAL	%DIFFERENCE
Mass of Deposits (g)	g	22.6	23.4	3.84
Ag ⁺ Removed	%	67.7	77.8	14.97
Cu ²⁺ Removed	%	33.3	34.1	2.43
Pb ²⁺ Removed	%	50.4	31.1	38.30
Fe ²⁺ Removed	%	40.7	-	-
Ag in Deposits	%	81.7	86.5	5.95
Cu in Deposits	%	1.68	2.10	24.41
Pb in Deposits	%	0.45	0.38	17.40
Fe in Deposits	%	0.74	-	-
Ag Recovered	%	50.3	57.6	14.6

The percent removal of silver ions from the effluent was 77.8 %, while the mass of the deposits were 23.44 grams, found to have silver purity of 86.54 %. The percent recovery of silver from the deposits was 57.64 %. Meanwhile, copper ion removal from the wastewater was found to be 34.08%. The values from experimental verification were within 15% difference from those predicted using the model equations, and the derived empirical equations for %Pb removal efficiency, and %Pb and %Cu deposited were up to ~38%. The deviations were due to considering a scale-up strategy in the absence of electroanalytical instruments. Further studies on potentiostatic electrodeposition can benefit with the inclusion of electroanalytical methods. Also, detailed parametric studies on the effects of pH, temperature, and electrode type on electrodeposition performance may be further investigated. More importantly, detailed theoretical modeling of the reaction mechanism involving multicomponent electrodeposition for complex wastewaters is still necessary.

3.7 Potentiostatic Silver Electrodeposition Charge Dose and Cost

Finally, the charge dose concept was employed to determine a scale-up parameter for potentiostatic electrodeposition. This parameter was also considered in previous electrodeposition scale-up studies for brine wastewater [54], algae-rich eutrophic lake water [55], and gold smelting wastewaters [6], [7]. This scale-up parameter is vital in estimating the energy requirement and operating cost of the process. Beyond the energy cost, a detailed process design and economic feasibility study of the potentiostatic electrodeposition process, in comparison with current gold smelting operations, will be covered in a future publication. Thus, the capital cost of the scaled-up electrodeposition equipment, and the annualized maintenance cost for electrode replacement were not considered in this study.

The charge dose parameter estimated from Equation 4 is applicable under constant-current or galvanostatic operations where changes in operating voltage are minimal. Thus, for potentiostatic electrodeposition, a modified approach was used to estimate the charge dose by considering the changes in current throughout the electrodeposition time. The applied charge [It] throughout the electrodeposition time was an integral function that can be numerically evaluated by calculating the area under the I vs t curve, as shown in the numerator function of Equation 11.

$$Q = \frac{\int_0^t I dt}{(C_0 - C) V_m} = \frac{\sum_{n=0}^t \frac{1}{2} (I_n + I_{n-1}) (t_n - t_{n-1})}{(C_0 - C) V_m} \quad (11)$$

A linear plot between applied charge and mass of silver ions removed was constructed to estimate the charge dose for the potentiostatic electrodeposition operation at 1.66 V and at an electrodeposition time of 72 minutes, as shown in **Figure 8**.

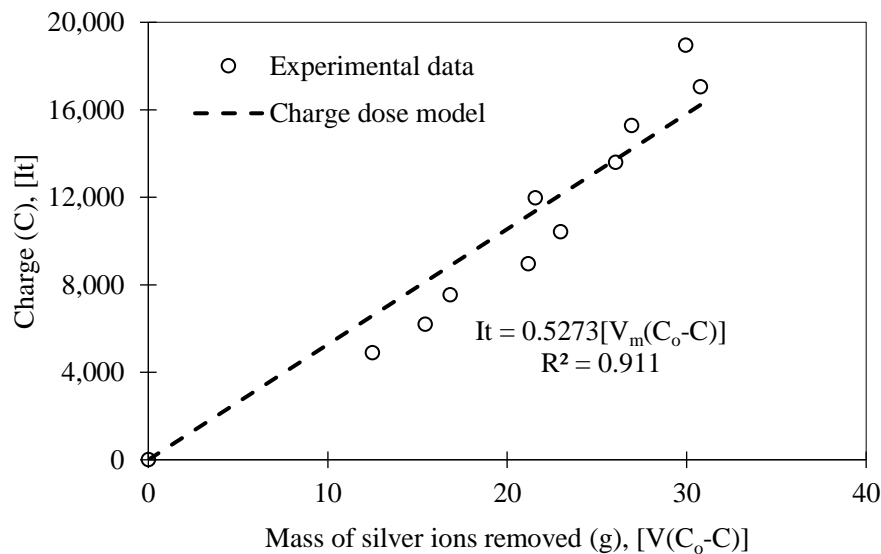


Figure 8. Estimated charge dose under potentiostatic electrodeposition: $E = 1.66$ V, $t_{\text{critical}} = 72$ mins, $C_o = 85,900$ mg/L

The charge dose evaluated at 1.66 V was 0.527 Coulombs per milligrams of silver ion removed from the gold smelting effluent with a high R-squared value of 0.911. This potentiostatic operating scale-up parameter was lower than that evaluated under galvanostatic or constant current electrodeposition evaluated by Alfafara, et al. at 1.273 C/mg silver ion removed [6]. This lower value favors the potentiostatic electrodeposition technique as less amount of electrical charge; hence, lower energy is needed in removing silver ions from the gold smelting effluent. In particular, using Equation 5, the estimated energy requirement for the operation was 0.24 kWh/kg silver removed, which was approximately more than half of that required in constant-current electrodeposition. Based on local industrial power cost of PhP 11.80 per kWh, the average treatment cost for silver electrodeposition was PhP 2.80 per kilogram of silver recovered. For an initial silver concentration of 85,900 mg/L, the

electrodeposition cost would approximately be PhP 240.5 per cubic meter of gold smelting wastewater. The direct proportion between the charge dose scale-up parameter and energy cost set a reasonable economic index for potentiostatic electrodeposition over the galvanostatic technique. Also, the purity of the recovered cathode deposits relative to silver was still higher during potentiostatic operation than that obtained using the galvanostatic method. At 1.66 V, the energy costs for the constant-voltage operation was half of that estimated by Alfafara et al. for a constant-current operation at 9 A. This cost reduction presents the potential advantage of the potentiostatic electrodeposition method.

IV. CONCLUSION

Potentiostatic or constant-voltage electrodeposition was investigated in contrast with galvanostatic or constant-current electrodeposition as a more practical method to recover silver from an artisanal gold smelting effluent. While previous studies on galvanostatic electrodeposition show high silver ion removal and recovery efficiencies, the potentiostatic electrodeposition technique favors recovery operations where high silver purity and minimum recovery costs are prioritized. Electrodeposition experiments showed that operating voltage proportionally affected the current supplied and influenced the deposition of dominant metal ions (silver, copper, iron, and lead), and initial rate of silver ion removal. The redissolution of metal deposits also occurred under high-potential electrodeposition (1.5 V to 2.0 V) based on the decreased mass of deposits recovered after prolonged operation. Critical operating conditions were essential in managing the co-deposition and simultaneous redissolution of deposits. Under a critical operating voltage of 1.33 V, the silver purity from recovered deposits was observed to be 89.33%, but at the expense of a low silver ion removal rate and longer electrodeposition time. On the other hand, high-potential electrodeposition (> 1.5 V) with the consideration of a critical electrodeposition time can minimize the metal redissolution but only to a certain extent. Numerical optimization with the aid of the statistical software revealed an optimum operating voltage of 1.66 V with a critical electrodeposition time of 72 minutes. Experimental verification resulting in 77.8% silver removal efficiency, and 86.5% silver purity, were found to be in reasonable agreement with predicted values. In both cases, silver purities were higher than those reported under constant-current electrodeposition. However, detailed parametric studies and the use of electroanalytical methods such as cyclic voltammetry are still recommended to understand the mechanisms of the competing electrochemical reactions like metal co-deposition, redissolution, and formation of metal sulfides. For scale-up, the charge dose evaluated for the potentiostatic electrodeposition was 0.5273 C/mg silver deposited with an energy requirement of 0.24 kWh/kg silver recovered. The corresponding cost was PhP 2.80 per kilogram of silver. Overall, the potentiostatic electrodeposition has lower energy consumption and cost than that of galvanostatic electrodeposition, and even those of copper recovery alternatives evaluated from previous studies. This lower operating cost is indicative of a favorable economic metrics that may be a subject of future process feasibility studies.

ACKNOWLEDGEMENTS

The authors acknowledge the financial support of the Office of Vice Chancellor for Research and Extension, University of the Philippines Los Baños through the Basic Research Program; the Department of Science and Technology through the Engineering Research and Development for Technology Faculty Research Grant; and Pure Earth Philippines. They also acknowledge the assistance of Resie Valderrama, Lorenz Fabro, Joel Villena of BIOTECH-UPLB, and Adriano Guevarra of Meycauayan, Bulacan.

NOMENCLATURE

Symbol	Description	Units
a	time constant	s
b	voltage constant	V
C_d	concentration of metal in acid-dissolved deposits	mg/L
C_o	initial metal ion concentration	mg/L
C	final metal ion concentration	mg/L
E	voltage or potential	V
I	Current	A
Q	charge dose	C/mg
t	electrodeposition time	s
$t_{critical}$	critical electrodeposition time	min
V_m	working volume for electrodeposition	L
V_s	volume of solution containing acid-dissolved cathode deposits	L
W_d	weight of the cathode deposits	mg

References

- [1] Pure Earth (Blacksmith Institute), "Annual Report 2008," New York, NY, 2008.
- [2] Pure Earth (Blacksmith Institute), "The World's Worst Polluted Places The Top Ten," 2007.
- [3] N. Espina, "Meycauayan, Marilao in World's 'Dirty 30' Report," *Philippine Daily Inquirer*, Manila, Philippines, pp. 16–17, 17-Sep-2007.
- [4] Greenpeace, "Hidden Consequences on people, planet and profit," Greenpeace International, The Netherlands, 2011.
- [5] Asian Development Bank, "Reduction of Mercury and Heavy Metals Contamination Resulting from Artisanal Gold Refining in Meycauayan, Bulacan River System," 2009.
- [6] C. Alfara *et al.*, "Scale-Up and Operating Factors for Electrolytic Silver Recovery from Effluents of Artisanal Used-Gold-Jewelry Smelting Plants in the Philippines," *J. Heal. Pollut.*, vol. 2, no. 3, pp. 32–42, 2012.
- [7] E. L. Vivas *et al.*, "Comparative evaluation of alkali precipitation and electrodeposition for copper removal in artisanal gold smelting wastewater in the Philippines," *Desalin. Water Treat.*, vol. 150, no. January, pp. 396–405, 2019.
- [8] D. Cervantes and R. Sapnu, "20 Bulacan gold smelters shut down," *Philippine Star*, San Fernando, Pampanga, 15-Oct-2000.
- [9] J. D. Hochmuth, J. Asselman, and K. A. C. De Schamphelaere, "Are interactive effects of harmful algal blooms and copper pollution a concern for water quality management?," *Water Res.*, vol. 60, pp. 41–53, 2014.
- [10] A. S. Lambert *et al.*, "Influence of temperature in pollution-induced community tolerance approaches used to assess effects of copper on freshwater phototrophic periphyton," *Sci. Total Environ.*, vol. 607–608, pp. 1018–1025, 2017.
- [11] P. P. Leal *et al.*, "Copper pollution exacerbates the effects of ocean acidification and warming on kelp microscopic early life stages," *Sci. Rep.*, vol. 8, no. 1, pp. 1–13, 2018.
- [12] R. I. Guaring and E. Espiritu, "Effects of heavy metals on Nile tilapia (*Oreochromis niloticus* L.)

- obtained from Meycauayan River, Philippines: Studies on health risks, bioaccumulation and oxidative stress," *Toxicol. Lett.*, vol. 295, no. 2018, p. S168, 2018.
- [13] M. D. Mendoza, "Application of Bioremediation in the Clean-up of the Marilao-Meycauayan-Obando River System in the Province of Bulacan," in *Addressing the Problems and Solutions of Environmental Pollution Through*, A. K. Raymundo, Ed. Manila, Philippines: National Science of Science and Technology, 2012, pp. 40–48.
- [14] E. Visco, J. M. Amparo, D. Torio, M. R. J. Atole, and M. Mendoza, "Integrated Adaptation Management Approach toward Sustained Fish Production by Fish Farmers of Marilao-Meycauayan-Obando River System," *Asian J. Agric. Dev.*, vol. 15, no. 1, pp. 61–73, 2018.
- [15] World Health Organization, "Copper in Drinking-water," 2004.
- [16] P. J. Landrigan and R. Fuller, "Environmental pollution: An enormous and invisible burden on health systems in low- and middle-income counties," *World Hosp. Health Serv.*, vol. 50, no. 4, pp. 35–40, 2014.
- [17] M. E. T. Mendoza, E. S. Visco, C. E. Jimena, J. S. Amparo, and M. D. Mendoza, "Knowledge, Attitudes and Practices Toward Toxic and Hazardous Substances: the Case of Selected Communities in," *Journal Nat. Stud.*, vol. 11, no. March 2017, pp. 1–18, 2012.
- [18] V. P. Migo, M. D. Mendoza, C. G. Alfafara, and J. M. Pulhin, "Industrial water use and the associated pollution and disposal problems in the Philippines," in *Global Issues in Water Policy*, vol. 8, A. C. Rola, J. M. Pulhin, and R. A. Hall, Eds. Springer International Publishing, 2018, pp. 87–116.
- [19] R. Dimeska, P. S. Murray, S. F. Ralph, and G. G. Wallace, "Electroless recovery of silver by inherently conducting polymer powders, membranes and composite materials," *Polymer (Guildf.)*, vol. 47, no. 13, pp. 4520–4530, 2006.
- [20] J. A. Murphy, A. H. Ackerman, and J. K. Heeren, "Recovery of silver from and some uses for waste silver chloride," *J. Chem. Educ.*, vol. 68, no. 7, pp. 602–604, 1991.
- [21] A. El Bachiri, A. Hagège, and M. Burgard, "Recovery of silver nitrate by transport across a liquid membrane containing dicyclohexano 18 crown 6 as a carrier," *J. Memb. Sci.*, vol. 121, no. 2, pp. 159–168, 1996.
- [22] P. P. Sun, H. Il Song, T. Y. Kim, B. J. Min, and S. Y. Cho, "Recovery of silver from the nitrate leaching solution of the spent Ag/ α -Al₂O₃ catalyst by solvent extraction," *Ind. Eng. Chem. Res.*, vol. 53, no. 52, pp. 20241–20246, 2014.
- [23] S. Park, D. W. Lee, J. C. Lee, and J. H. Lee, "Photocatalytic silver recovery using ZnO nanopowders synthesized by modified glycine-nitrate process," *J. Am. Ceram. Soc.*, vol. 86, no. 9, pp. 1508–1512, 2003.
- [24] S. S. V Tatiparti and F. Ebrahimi, "Potentiostatic versus galvanostatic electrodeposition of nanocrystalline Al-Mg alloy powders," *J. Solid State Electrochem.*, vol. 16, no. 3, pp. 1255–1262, 2012.
- [25] H. B. Kim, H. Kim, H. S. Sohn, I. Son, and H. S. Lee, "Effect of pH on the morphological evolution of NiO thin film synthesized on ZnO nanorod arrays by electrodeposition and post-annealing," *Mater. Lett.*, vol. 101, pp. 65–68, 2013.
- [26] R. C. M. Salles, G. C. G. De Oliveira, S. L. Díaz, O. E. Barcia, and O. R. Mattos, "Electrodeposition of Zn in acid sulphate solutions: PH effects," *Electrochim. Acta*, vol. 56, no. 23, pp. 7931–7939, 2011.
- [27] C. Srivastava et al., "Effect of pH on anomalous co-deposition and current efficiency during electrodeposition of Ni-Zn-P alloys," *Surf. Coatings Technol.*, vol. 313, pp. 8–16, 2017.
- [28] R. Valaski, S. Ayoub, L. Micaroni, and I. A. Hümmelgen, "The influence of electrode material on charge transport properties of polypyrrole thin films," *Thin Solid Films*, vol. 388, no. 1–2, pp. 171–176, 2001.
- [29] L. Vieira, R. Schennach, and B. Gollas, "The effect of the electrode material on the electrodeposition of zinc from deep eutectic solvents," *Electrochim. Acta*, vol. 197, pp. 344–352, 2016.
- [30] C. Özmetin, "A rotating disc study on silver dissolution in concentrate HNO₃ solutions," *Chem. Biochem. Eng. Q.*, vol. 17, no. 2, pp. 165–169, 2003.
- [31] G. A. M. Ali, M. M. Yusoff, Y. H. Ng, H. N. Lim, and K. F. Chong, "Potentiostatic and galvanostatic electrodeposition of manganese oxide for supercapacitor application: A comparison study," *Curr. Appl. Phys.*, vol. 15, no. 10, pp. 1143–1147, 2015.
- [32] M. A. A. Mohd Abdah, N. S. Mohd Razali, P. T. Lim, S. Kulandaivalu, and Y. Sulaiman, "One-step potentiostatic electrodeposition of polypyrrole/graphene oxide/multi-walled carbon nanotubes ternary nanocomposite for supercapacitor," *Mater. Chem. Phys.*, vol. 219, no. June, pp. 120–128, 2018.
- [33] Y. Ni, Y. Zhang, and J. Hong, "Potentiostatic electrodeposition route for quick synthesis of featherlike

- PbTe dendrites: Influencing factors and shape evolution,” *Cryst. Growth Des.*, vol. 11, no. 6, pp. 2142–2148, 2011.
- [34] Y. Yang, Y. Li, and M. Pritzker, “Control of Cu₂O Film Morphology Using Potentiostatic Pulsed Electrodeposition,” *Electrochim. Acta*, vol. 213, pp. 225–235, 2016.
- [35] O. Shimamura, N. Yoshimoto, M. Matsumoto, M. Egashia, and M. Morita, “Electrochemical co-deposition of magnesium with lithium from quaternary ammonium-based ionic liquid,” *J. Power Sources*, vol. 196, no. 3, pp. 1586–1588, 2011.
- [36] I. Sultana *et al.*, “Electrodeposition of silver (Ag) nanoparticles on MnO₂ nanorods for fabrication of highly conductive and flexible paper electrodes for energy storage application,” *J. Mater. Sci. Mater. Electron.*, vol. 29, no. 24, pp. 20588–20594, 2018.
- [37] B. R. Cruz-Ortiz, M. A. Garcia-Lobato, E. R. Larios-Durán, E. M. Múzquiz-Ramos, and J. C. Ballesteros-Pacheco, “Potentiostatic electrodeposition of nanostructured NiO thin films for their application as electrocatalyst,” *J. Electroanal. Chem.*, vol. 772, pp. 38–45, 2016.
- [38] I. M. Sasidharan Pillai and A. K. Gupta, “Potentiostatic electrodeposition of a novel cost effective PbO₂ electrode: Degradation study with emphasis on current efficiency and energy consumption,” *J. Electroanal. Chem.*, vol. 749, pp. 16–25, 2015.
- [39] K. K. Abdugaffarova, M. V. Dorogov, A. A. Vikarchuk, and I. S. Yasnikov, “Evolution of the morphology of small pentagonal particles and microcrystals during the electrodeposition of silver in a potentiostatic regime,” *Bull. Russ. Acad. Sci. Phys.*, vol. 81, no. 11, pp. 1327–1329, 2017.
- [40] C. Das and K. R. Balasubramaniam, “Structural and morphological studies of cuprous oxide thin film developed via. potentiostatic electrodeposition,” *2014 IEEE 40th Photovolt. Spec. Conf. PVSC 2014*, pp. 254–256, 2014.
- [41] G. M. Lohar *et al.*, “Photoelectrochemical cell studies of Fe²⁺ doped ZnSe nanorods using the potentiostatic mode of electrodeposition,” *J. Colloid Interface Sci.*, vol. 458, pp. 136–146, 2015.
- [42] M. Mikolasek *et al.*, “Potentiostatic electrodeposition of Cu₂O under light and dark for photoelectrochemical hydrogen generation applications,” *Adv. Electr. Electron. Eng.*, vol. 16, no. 3, pp. 367–373, 2018.
- [43] T. Yang, Y. Ding, C. Li, N. Yin, X. Liu, and P. Li, “Potentiostatic and galvanostatic two-step electrodeposition of semiconductor Cu₂O films and its photovoltaic application,” *J. Alloys Compd.*, vol. 727, pp. 14–19, 2017.
- [44] L. S. Clesceri, A. E. Greenberg, and A. D. Eaton, *Standard methods for the examination of water and wastewater*. California: American Public Health Association, American Water Works Association, Water Environment Federation, 1998.
- [45] M. D. Adams, *Advances in Gold Ore Processing*. Elsevier, 2005.
- [46] D. R. Lide, *Handbook of Chemistry and Physics*, 85th Editi. Cleveland, Ohio: CRC Press, 2003.
- [47] V. B. Prabhune, N. S. Shinde, and V. J. Fulari, “Studies on electrodeposited silver sulphide thin films by double exposure holographic interferometry,” *Appl. Surf. Sci.*, vol. 255, no. 5 PART 1, pp. 1819–1823, 2008.
- [48] S. Omeiri, B. Hadjarab, and M. Trari, “Photoelectrochemical properties of anodic silver sulphide thin films,” *Thin Solid Films*, vol. 519, no. 13, pp. 4277–4281, 2011.
- [49] K. Kim, E. Lee, I. Choi, J. Yoo, and H. Park, “Electrolysis of nitric acid by using a glassy carbon fiber column electrode system,” *J. Radioanal. Nucl. Chem.*, vol. 245, no. 2, pp. 301–308, 2000.
- [50] D. Siesic, F. Balbaud-céliér, and B. Tribollet, “Mechanism of Nitric Acid Reduction and Kinetic Modelling,” pp. 6174–6184, 2014.
- [51] A. S. Elmezayyen, S. Guan, F. M. Reicha, I. M. El-Sherbiny, J. Zheng, and C. Xu, “Effect of conductive substrate (working electrode) on the morphology of electrodeposited Cu₂O,” *J. Phys. D. Appl. Phys.*, vol. 48, no. 17, 2015.
- [52] H. S. Fogler, *Elements of Chemical Reaction Engineering*, Fifth edit. New York: Prentice Hall, 2016.
- [53] I. Hanafi, A. Razak, and S. Radiman, “Potentiostatic electrodeposition of Co-Ni-Fe thin films from sulfate medium,” *J. Chem. Technol. Metall.*, vol. 51, no. 5, pp. 547–555, 2016.
- [54] C. G. Alfafara, T. Kawamori, N. Nomura, M. Kiuchi, and M. Matsumura, “Electrolytic removal of ammonia from brine wastewater: Scale-up, operation and pilot-scale evaluation,” *J. Chem. Technol. Biotechnol.*, vol. 79, no. 3, pp. 291–298, 2004.
- [55] C. G. Alfafara, K. Nakano, N. Nomura, T. Igarashi, and M. Matsumura, “Operating and scale-up factors for the electrolytic removal of algae from eutrophied lakewater,” *J. Chem. Technol. Biotechnol.*, vol. 77, no. 8, pp. 871–876, 2002.